photochem

MDPI

Article

Phosphorescence and Photophysical Parameters of Porphycene in Cryogenic Matrices

Barbara Golec [1], Aleksander Gorski [1] and Jacek Waluk [1,2,*]

[1] Institute of Physical Chemistry, Polish Academy of Sciences, Kasprzaka 44/52, 01-224 Warsaw, Poland; bgolec@ichf.edu.pl (B.G.); agorski@ichf.edu.pl (A.G.)
[2] Faculty of Mathematics and Science, Cardinal Stefan Wyszyński University, Dewajtis 5, 01-815 Warsaw, Poland
* Correspondence: jwaluk@ichf.edu.pl; Tel.: +48-22-343-3332

Abstract: Matrix isolation studies were carried out for porphycene, an isomer of porphyrin, embedded in solid nitrogen and xenon. The external heavy atom effect resulted in nearly a 100% population of the triplet state and in the appearance of phosphorescence, with the origin located at 10163 cm^{-1}. This energy is much lower than that corresponding to the T_1 position in porphyrin. This difference could be explained by postulating that the orbital origin corresponds in both isomers to the second excited singlet state, which lies much closer to S_1 in porphycene. Most of the vibrational frequencies observed in the phosphorescence spectrum correspond to totally symmetric modes, but several ones were assigned to the out-of-plane Bg vibrations. These bands are not observed in fluorescence, which suggests their possible role in vibronic-spin-orbit coupling.

Keywords: phosphorescence; triplet state origin; singlet-triplet energy gap; vibrational frequencies; porphyrin isomers

check for updates

Citation: Golec, B.; Gorski, A.; Waluk, J. Phosphorescence and Photophysical Parameters of Porphycene in Cryogenic Matrices. *Photochem* **2022**, *2*, 217–224. https://doi.org/10.3390/photochem2010016

Academic Editors: Gulce Ogruc Ildiz and Licinia L. G. Justino

Received: 22 February 2022
Accepted: 7 March 2022
Published: 9 March 2022

Publisher's Note: MDPI stays neutral with regard to jurisdictional claims in published maps and institutional affiliations.

Copyright: © 2022 by the authors. Licensee MDPI, Basel, Switzerland. This article is an open access article distributed under the terms and conditions of the Creative Commons Attribution (CC BY) license (https://creativecommons.org/licenses/by/4.0/).

1. Introduction

The detailed characterization of the photophysical characteristics of a chromophore is a prerequisite for successful applications. In particular, the properties of the triplet state, such as its energy, yield of formation via intersystem crossing from the singlet state, lifetime, and the ability to generate singlet oxygen, are crucial when designing new materials, e.g., photosensitizers, photovoltaic cells, or light emitting diodes. Moreover, the triplet state parameters often determine the photostability of a molecule, since photodegradation usually involves the triplet state. It is therefore not surprising that large databases containing triplet state data are available for many popular chromophores [1]. One of them is porphyrin, justly called "pigment of life" [2]. In most porphyrins, the yield of S_1-T_1 intersystem crossing is high, exceeding 70–80%. The S_1-T_1 energy separation is about 3500 cm^{-1}. Investigations of parent, unsubstituted porphyrin in xenon matrices yielded values of 3683 and 3687 cm^{-1}, determined from the difference between the origins of absorption [3] and phosphorescence [4] of the two main sites observed in this environment. The triplet lifetimes in argon and xenon, 2.6 and 0.63 ms, respectively [4], are not much different, but the radiative constant of the triplet depopulation dramatically increases in the heavy atom matrix, which allows for the registration of vibronically resolved phosphorescence in the not so readily accessible spectral region of 8000–13,000 cm^{-1}.

Porphycene (Pc)—a structural isomer of porphyrin (Pr) (Scheme 1)—has gained much attention as a model for understanding single and double hydrogen transfer in the ground and electronically excited states [5] and as a promising agent for photodynamic therapy of cancer [6] and photoinactivation of bacteria [7]. Spectral and photophysical data for parent, unsubstituted porphycene and its derivatives are quite rich regarding the singlet state properties, but much less is known about the triplet characteristics. The triplet formation efficiency is lower than in porphyrin [5,8]. Moreover, it can be reduced practically to zero

by multiple substitutions at the meso positions [9]. The triplet lifetimes, measured in solution [10,11] or lipid vesicles [12], are of the order of tens of microseconds. The triplet energies are considerably lower than in porphyrin (ca. 10,000 vs. 12,500 cm^{-1}). They were determined for several porphycenes from the emission studies in the near IR region, carried out at room temperature in degassed iodopropane solutions [13]; no spectra have been presented. For the parent porphycene, Nonell et al. reported the phosphorescence by comparing the emission in degassed and aerated bromobenzene solutions at room temperature [14]. The spectrum consisted of two broad bands, centered around 1000 and 1150 nm.

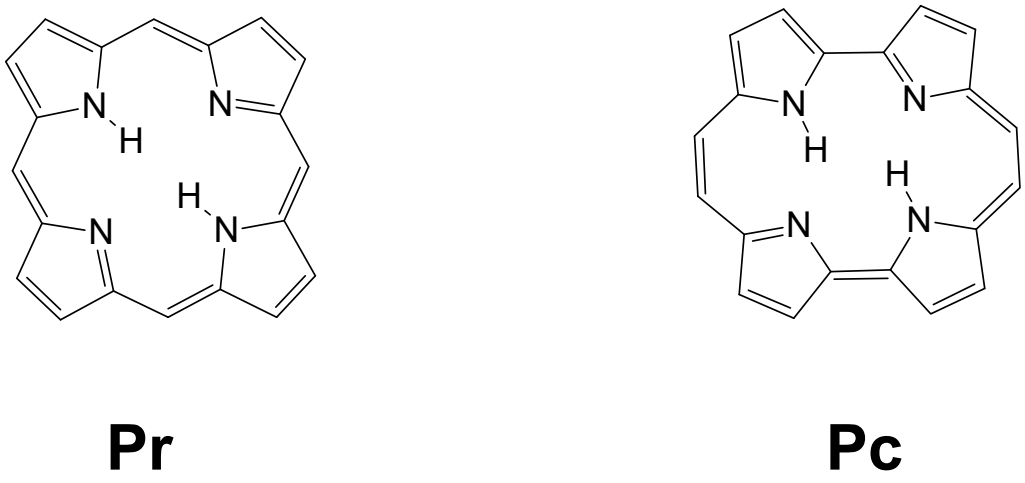

Scheme 1. (**Left**), porphyrin (porphine); (**right**), porphycene.

To the best of our knowledge, no vibrationally resolved phosphorescence spectra of porphycenes have been published so far. The goal of our work was to obtain such a spectrum by placing the chromophore in a rare gas matrix. Based on previous observations, xenon was used, in order to enhance the triplet formation yield and, possibly, to increase the radiative constant of T_1 depopulation. Next, in order to quantitatively study the external heavy atom effect, we measured the spectra in solid nitrogen. Triplet and singlet lifetimes as well as triplet formation efficiencies were compared for both matrices. Finally, we also performed quantum chemical calculations for porphyrin and porphycene, in order to understand the differences in singlet-triplet energy gaps and to assign the orbital origin of the triplet state.

2. Materials and Methods

Porphycene was synthesized and purified as described previously [15].

Nitrogen and xenon matrices were prepared on a sapphire deposition window attached to the cold finger of a closed-cycle helium cryostat (Displex 202, Advance Research Systems). Porphycene was sublimed into the rare gas by heating up to 390 K. The deposition window was kept at 10 K and 57 K during the deposition of nitrogen and xenon matrices, respectively.

Phosphorescence was measured with a home-made spectrometer based on a BENTHAM DTMc300 double monochromator equipped with a TE cooled photomultiplier (Hamamatsu H10330C-75, 950–1700 nm registration range). Two different laser sources have been used for excitation: (i) a Powerchip 355 nm Laser (Teem Photonics) and (ii) a CW ring laser (Coherent 899), pumped by an argon laser (Coherent Innova 300).

Steady state fluorescence spectra and fluorescence decays were obtained using an Edinburgh FS 900 CDT / FL 900 CDT fluorometer (Edinburgh Analytical Instruments). A NanoLED diode (297 nm, 1 MHz repetition rate) was used for time-resolved measurements.

Absorption spectra were recorded using a Shimadzu UV2700 spectrophotometer.

Calculations were performed using the density functional theory (DFT) and its time-dependent variant (TD DFT), as implemented in the Amsterdam Modeling Suite (version 2021.10-4) [16]. BP86-D functional [17,18] and TZP basis set were used in these simulations.

3. Results and Discussion

Figure 1 shows the absorption spectra of Pc obtained for nitrogen and xenon matrices. The absorption of matrix-isolated Pc has been studied in detail before [19–22]. The presently obtained spectra are similar to the reported ones. The linewidths are somewhat narrower than in the previously published works, which enables a better resolution of a characteristic multiple-site structure observed in nitrogen. In contrast, only one dominant site, exhibiting a larger bandwidth, is observed for the xenon environment. Transitions to both S_1 and S_2 are red-shifted in xenon, by 180 and 230 cm^{-1}, respectively. This leads to the S_1-S_2 energy separation of 887 cm^{-1} in nitrogen and 837 cm^{-1} in xenon. The S_1-S_2 energy gap is thus significantly—nearly four times—smaller than in porphyrin, for which the reported values are about 3270 cm^{-1} (in argon) and 3100 cm^{-1} (in xenon).

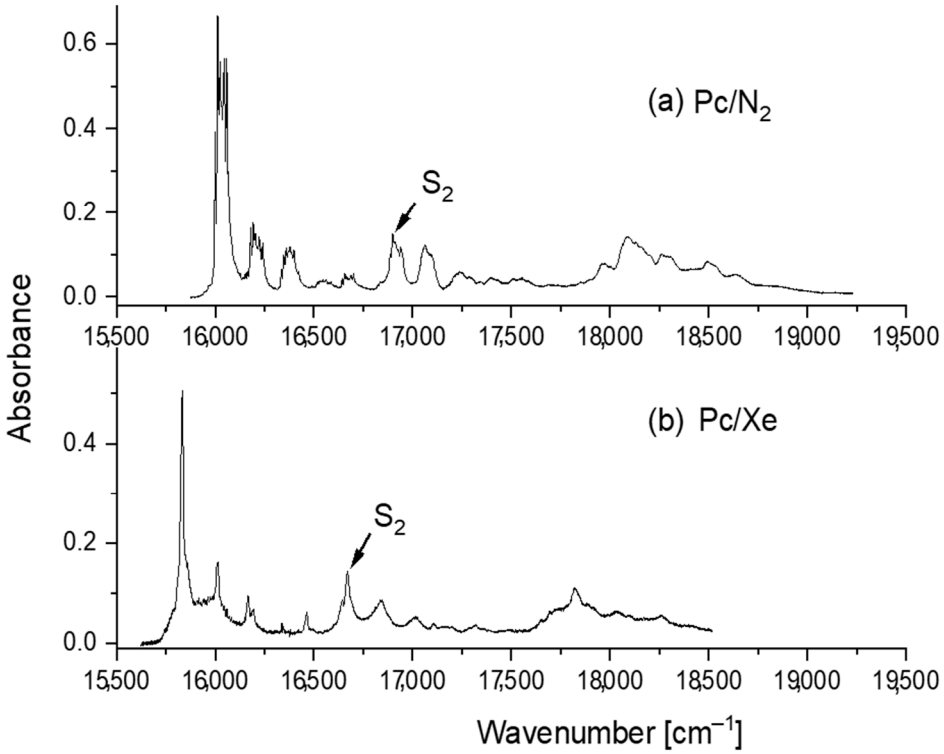

Figure 1. Absorption of Pc in (**a**) nitrogen and (**b**) xenon matrices. T = 10 K. The arrows mark the origin of the S_0-S_2 electronic transition.

Fluorescence spectra are shown in Figure 2. This experiment was performed with a broad excitation and low spectral resolution, so that the site structure is no longer observed. The purpose was to compare the intensities in both cases. The emission was much stronger in nitrogen. The relative quantum yields were estimated from the fluorescence decay times measured for both samples. Such a procedure assumes similar values of radiative decay constants in different environments, which has been demonstrated for porphycene [23]. The lifetime of fluorescence (τ_F) in the nitrogen matrix, 21 ns, was 60 times longer than that measured for the xenon environment (Table 1). The fluorescence lifetimes of Pc measured in room temperature solutions are about 10 ns, whereas the quantum yields vary, depending on the solvent, between 0.39 and 0.50 [23]. This would suggest a rather low triplet formation efficiency in nitrogen. The experimentally obtained value is 0.36. On the other hand, the value obtained for the sample in xenon is practically 1, as could have been expected based on the dramatic shortening of the S_1 lifetime caused by the external heavy atom effect.

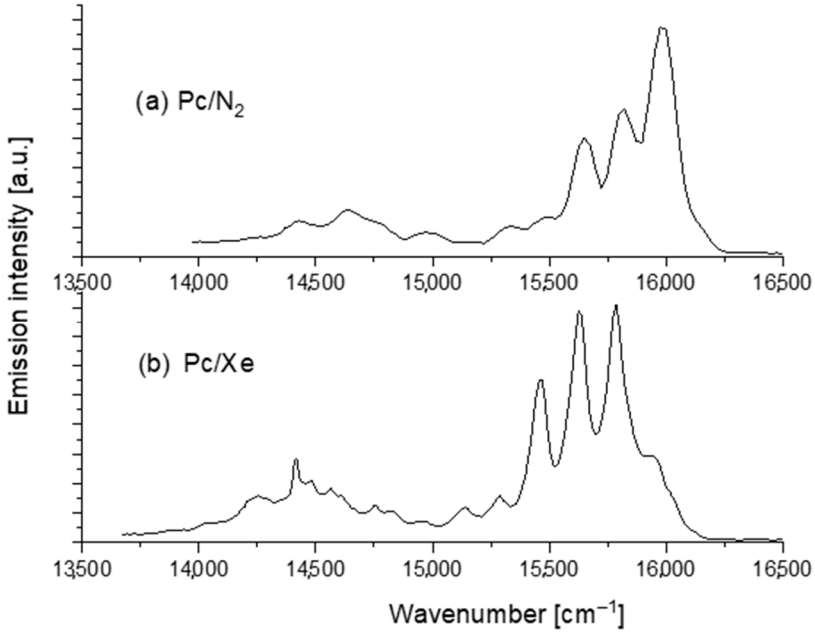

Figure 2. Fluorescence of Pc in (**a**) nitrogen and (**b**) xenon matrices. T = 10 K. Excitation wavelengths: (**a**) 370 nm and (**b**) 560 nm.

Table 1. Photophysical parameters of Pc in N_2 and Xe matrices.

	τ_F, ns	τ_T, μs	Φ_T
N_2	21 ± 2	2000 ± 40	0.36 ± 0.04
Xe	0.35 ± 0.1	45 ± 0.5	1 ± 0.05

The triplet decays reveal the opposite behavior (Table 1). The ratio of T_1 lifetimes (τ_T), (2000 μs (N_2))/(45 μs (Xe)) is not much different from what is observed for the changes in the $T_1 \leftarrow S_1$ intersystem crossing rates. Interestingly, while the T_1 lifetimes are very similar for Pr in argon and Pc in nitrogen, in xenon it is the Pc triplet that decays much faster. A possible explanation is the larger value of the radiative constant of triplet depopulation in Pc. One should remember that the transition to the S_1 state is much weaker in Pr than in Pc.

While the phosphorescence was extremely weak in nitrogen-isolated Pc, it could be readily obtained in xenon matrices (Figure 3). The electronic ground state vibrational frequencies extracted from the phosphorescence spectrum are presented in Table 2. The same table also contains the frequencies previously obtained from the fluorescence of Pc in xenon. Because of the better spectral resolution in the present case, we could observe and assign additional lines, such as combinations of low frequency modes with the strong transition observed at 1554 cm^{-1} (29 Ag). The assignments in Table 2 are based on our previous work that included frequencies obtained from IR, Raman, fluorescence, and inelastic neutron scattering data combined with quantum chemical calculations and isotopic substitution [24].

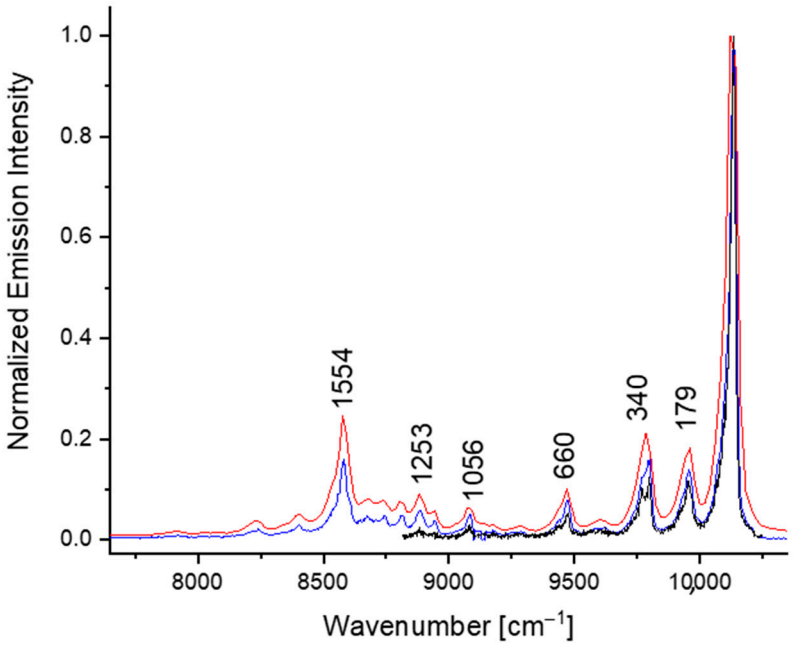

Figure 3. Phosphorescence of Pc in xenon matrices measured at three different spectral resolutions. T = 10 K. Excitation wavelength: 631.6 nm, corresponding to the location of the main site (see Figure 1b).

Most of the features present in the phosphorescence have their counterparts in the fluorescence spectrum. However, in contrast to fluorescence, which reveals only totally symmetric (Ag) modes, several bands in phosphorescence are assigned to out-of-plane Bg vibrations. This indicates a possible contribution of the vibronic-spin-orbit coupling mechanism [25] to the phosphorescence intensity.

Using the luminescence data available for both chromophores, we are now ready to compare the pattern of low-lying electronic states in Pc and Pr. The most conspicuous difference is the S_1-T_1 energy gap. While the origins of the S_0-S_1 transitions differ by less than 500 cm^{-1} (16,270 cm^{-1} in Pr vs. 15,821 cm^{-1} in Pc), the T_1 state in Pc is located at an energy that is lower by nearly 2500 cm^{-1} with respect to Pr (10,134 vs. 12,588 cm^{-1}). An opposite behavior is found for the relative positions of S_1 and S_2 in the two chromophores. The energy difference between the transitions to S_1 (Q_x) and S_2 (Q_y) in a xenon matrix exceeds 3100 cm^{-1} in porphyrin [4], whereas in porphycene it amounts to only 838 cm^{-1} [19].

We postulate that the lowering of the S_2 energy upon going from Pr to Pc is responsible for the large stabilization of the lowest triplet state in the latter. Calculations suggest that, in both molecules, the lowest triplet state is well described by the same electronic configuration, involving the HOMO–LUMO electron jump (Table 3). Such a configuration is dominant, for both Pr and Pc, in the S_0-S_2 transition, but not in S_0-S_1. This implies a larger singlet-triplet splitting for S_2. Assuming a similar value of the singlet-triplet splitting in both chromophores, one would expect a difference in the T_1 location corresponding to the difference in S_2 energies. This is indeed observed experimentally: the T_1 energies differ by ca. 2500 cm^{-1}, the energies of S_2 by ca. 2700 cm^{-1}.

Table 2. Vibrational frequencies (in cm^{-1}) observed in phosphorescence in xenon, compared with the previously reported data [19] obtained from fluorescence in the same matrix.

Phosphorescence	Fluorescence	Assignment [a]
179	184	2 Ag
340	336	3 Ag
368	358	4 Ag
511	510	2 Ag + 3 Ag
541	538	2 Ag + 4 Ag
621		7 Bg
660	665	7 Ag
	686	2 × 3 Ag
696		9 Bg
	703	3 Ag + 4 Ag
	723	2 × 4 Ag
847		1 Ag + 7 Bg
	863	9 Ag
881		14 Bg
959	961	10 Ag
	1010	3 × 3 Ag
1056		14 Ag
	1079	3 × 4 Ag
1192	1203	17 Ag
1253	1265	19 Ag
1322		20 Ag
	1354	21 Ag
1392	1395	23 Ag
1426		25 Ag
1458		26 Ag
1486	1497	27 Ag
1554	1562	29 Ag
	1585	
	1614	30 Ag
1730		2 Ag + 29 Ag
1891		3 Ag + 29 Ag
1918		4 Ag + 29 Ag
2215		7 Ag + 29 Ag

[a] based on ref. [24].

Table 3. Calculated transition energies.

	S_1	S_2	T_1	T_2
Pc	17,191 [a]	18,226	11,898	12,449
	(0.0927) [b]	(0.1549)		
	54.4.% sH-L [c]	56.3% H-L	H-L	sH-L
	26% H-L	25.0% sH-L		
Pr	17,505 (0.0007)	18,563 (0.0004)	14,087	14,870
	61.5% H-sL	57.3% H-L		
	37.5% sH-L	41.4% sH-sL	H-L	H-sL

[a] cm^{-1}; [b] oscillator strength in parentheses; [c] dominant configurations; H, sH: highest and second highest occupied molecular orbital; L, sL: lowest and second lowest unoccupied molecular orbital.

The calculations accurately predict the difference in the triplet energies of Pr and Pc, (2200 cm^{-1} vs. 2500 cm^{-1} obtained in the experiment). They also correctly reproduce the lower energy of S_1 in Pc (300 cm^{-1} vs. the observed value of 450 cm^{-1}). The S_1-S_2 separation is well reproduced for Pc, but for the S_2 state both the energy and the oscillator strength (relative to those of S_1) are predicted rather poorly.

4. Summary

Electronic spectroscopy studies of porphycene embedded in xenon matrices enabled an accurate determination of the location of the lowest triplet state. The vibronically resolved phosphorescence was recorded, exhibiting, in contrast to fluorescence, not only totally symmetric modes. The triplet location in porphycene is significantly red-shifted compared to porphyrin. This was explained by assigning the T_1 orbital origin to that of S_2, a state which is strongly stabilized with respect to S_1 upon passing from Pr to Pc.

In view of the crucial role the triplet state plays in various photophysical, photochemical, and photochemical processes, more detailed studies seem worthwhile, focusing on such issues as, e.g., substituent effects that could lead to the inversion of the two lowest lying triplet states in porphyrin and its isomers. Several relatively old papers suggest for Pr that the T_1 and T_2 states lie very close to each other and that their ordering may depend on the environment [4,26–29]. The same may be true for porphycene, as suggested by the calculated T_1-T_2 energy gap, which is even smaller than in porphyrin (Table 3).

Author Contributions: Conceptualization, J.W.; software, J.W.; formal analysis, B.G., A.G. and J.W.; investigation, B.G. and A.G.; writing—original draft preparation, J.W. All authors have read and agreed to the published version of the manuscript.

Funding: This research was funded by the Polish National Science Centre, grant numbers 2016/22/A/ST4/00029 and 2020/39/B/ST4/01956.

Data Availability Statement: Data is contained within the article.

Conflicts of Interest: The authors declare no conflict of interest.

References

1. Montalti, M.; Credi, A.; Prodi, L.; Gandolfi, M.T. *Handbook of Photochemistry*, 3rd ed.; Montalti, M., Credi, A., Prodi, L., Gandolfi, M.T., Eds.; Taylor & Francis Group: Abingdon, UK, 2006.
2. Battersby, A.R. Tetrapyrroles: The Pigments of Life. *Nat. Prod. Rep.* **2000**, *17*, 507–526. [CrossRef] [PubMed]
3. Radziszewski, J.; Waluk, J.; Michl, J. FT Visible Absorption Spectroscopy of Porphine in Noble Gas Matrices. *J. Mol. Spectrosc.* **1990**, *140*, 373–389. [CrossRef]
4. Radziszewski, J.G.; Waluk, J.; Nepraš, M.; Michl, J. Fourier Transform Fluorescence and Phosphorescence of Porphine in Rare Gas Matrices. *J. Phys. Chem.* **1991**, *95*, 1963–1969. [CrossRef]
5. Waluk, J. Spectroscopy and Tautomerization Studies of Porphycenes. *Chem. Rev.* **2017**, *117*, 2447–2480. [CrossRef] [PubMed]
6. Stockert, J.C.; Cañete, M.; Juarranz, A.; Villanueva, A.; Horobin, R.W.; Borrell, J.; Teixidó, J.; Nonell, S. Porphycenes: Facts and Prospects in Photodynamic Therapy of Cancer. *Curr. Med. Chem.* **2007**, *14*, 997–1026. [CrossRef]
7. Polo, L.; Segalla, A.; Bertoloni, G.; Jori, G.; Schaffner, K.; Reddi, E. Polylysine-Porphycene Conjugates as Efficient Photosensitizers for the Inactivation of Microbial Pathogens. *J. Photochem. Photobiol. B Biol.* **2000**, *59*, 152–158. [CrossRef]
8. Planas, O.; Gallavardin, T.; Nonell, S. Unusual Properties of Asymmetric Porphycenes. In *Handbook of Porphyrin Science*; Kadish, K.M., Smith, K.M., Guilard, R., Eds.; World Scientific: Singapore, 2016; Volume 41, pp. 299–349.
9. Gil, M.; Dobkowski, J.; Wiosna-Sałyga, G.; Urbańska, N.; Fita, P.; Radzewicz, C.; Pietraszkiewicz, M.; Borowicz, P.; Marks, D.; Glasbeek, M.; et al. Unusual, Solvent Viscosity-Controlled Tautomerism and Photophysics: Meso-Alkylated Porphycenes. *J. Am. Chem. Soc.* **2010**, *132*, 13472–13485. [CrossRef]
10. Aramendia, P.F.; Redmond, R.W.; Nonell, S.; Schuster, W.; Braslavsky, S.E.; Schaffner, K.; Vogel, E. The Photophysical Properties of Porphycenes: Potential Photodynamic Therapy Agents. *Photochem. Photobiol.* **1986**, *44*, 555–559. [CrossRef]
11. Levanon, H.; Toporowicz, M.; Ofir, H.; Fessenden, R.W.; Das, P.K.; Vogel, E.; Köcher, M.; Pramod, K. Triplet-State Formation of Porphycenes—Intersystem Crossing Versus Sensitization Mechanisms. *J. Phys. Chem.* **1988**, *92*, 2429–2433. [CrossRef]
12. Redmond, R.W.; Valduga, G.; Nonell, S.; Braslavsky, S.E.; Schaffner, K.; Vogel, E.; Pramod, K.; Köcher, M. The Photophysical Properties of Porphycene Incorporated in Small Unilamellar Lipid Vesicles. *J. Photochem. Photobiol. B Biol.* **1989**, *3*, 193–207. [CrossRef]
13. Braslavsky, S.E.; Müller, M.; Mártire, D.O.; Pörting, S.; Bertolotti, S.G.; Chakravorti, S.; Koç-Weier, G.; Knipp, B.; Schaffner, K. Photophysical Properties of Porphycene Derivatives (18 π Porphyrinoids). *J. Photochem. Photobiol. B Biol.* **1997**, *40*, 191–198. [CrossRef]
14. Nonell, S.; Aramendía, P.F.; Heihoff, K.; Negri, R.M.; Braslavsky, S.E. Laser-Induced Optoacoustics Combined with near-Infrared Emission. An Alternative Approach for the Determination of Intersystem Crossing Quantum Yields Applied to Porphycenes. *J. Phys. Chem.* **1990**, *94*, 5879–5883. [CrossRef]
15. Urbańska, N.; Pietraszkiewicz, M.; Waluk, J. Efficient Synthesis of Porphycene. *J. Porphyr. Phthalocyanines* **2007**, *11*, 596–600. [CrossRef]

16. te Velde, G.; Bickelhaupt, F.M.; Baerends, E.J.; Fonseca Guerra, C.; van Gisbergen, S.J.A.; Snijders, J.G.; Ziegler, T. Chemistry with ADF. *J. Comput. Chem.* **2001**, *22*, 931–967. [CrossRef]
17. Becke, A.D. Density-Functional Exchange-Energy Approximation with Correct Asymptotic Behavior. *Phys. Rev. A* **1988**, *38*, 3098–3100. [CrossRef]
18. Perdew, J.P. Density-Functional Approximation for the Correlation Energy of the Inhomogeneous Electron Gas. *Phys. Rev. B* **1986**, *33*, 8822–8824, Erratum: Density-Functional Approximation for the Correlation Energy of the Inhomogeneous Electron Gas. *Phys. Rev. B* **1986**, *34*, 7406–7406. [CrossRef]
19. Starukhin, A.; Vogel, E.; Waluk, J. Electronic Spectra in Porphycenes in Rare Gas and Nitrogen Matrices. *J. Phys. Chem. A* **1998**, *102*, 9999–10006. [CrossRef]
20. Kyrychenko, A.; Waluk, J. Molecular Dynamics Simulations of Matrix Deposition. Iii. Site Structure Analysis for Porphycene in Argon and Xenon. *J. Chem. Phys.* **2005**, *123*, 064706. [CrossRef]
21. Kyrychenko, A.; Gawinkowski, S.; Urbańska, N.; Pietraszkiewicz, M.; Waluk, J. Matrix Isolation Spectroscopy and Molecular Dynamics Simulations for 2,7,12,17-Tetra-Tert-Butylporphycene in Argon and Xenon. *J. Chem. Phys.* **2007**, *127*, 134501. [CrossRef]
22. Gil, M.; Gorski, A.; Starukhin, A.; Waluk, J. Fluorescence Studies of Porphycene in Various Cryogenic Environments. *Low Temp. Phys.* **2019**, *45*, 656–662. [CrossRef]
23. Kijak, M.; Nawara, K.; Listkowski, A.; Masiera, N.; Buczyńska, J.; Urbańska, N.; Orzanowska, G.; Pietraszkiewicz, M.; Waluk, J. 2+2 Can Make Nearly a Thousand! Comparison of Di- and Tetra-Meso-Alkyl-Substituted Porphycenes. *J. Phys. Chem. A* **2020**, *124*, 4594–4604. [CrossRef] [PubMed]
24. Gawinkowski, S.; Walewski, Ł.; Vdovin, A.; Slenczka, A.; Rols, S.; Johnson, M.R.; Lesyng, B.; Waluk, J. Vibrations and Hydrogen Bonding in Porphycene. *Phys. Chem. Chem. Phys.* **2012**, *14*, 5489–5503. [CrossRef] [PubMed]
25. Penfold, T.J.; Gindensperger, E.; Daniel, C.; Marian, C.M. Spin-Vibronic Mechanism for Intersystem Crossing. *Chem. Rev.* **2018**, *118*, 6975–7025. [CrossRef] [PubMed]
26. van Dorp, W.G.; Soma, M.; Kooter, J.A.; van der Waals, J.H. Electron Spin Resonance in the Photo-Excited Triplet State of Free Base Porphin in a Single Crystal of *n*-Octane. *Mol. Phys.* **1974**, *28*, 1551–1568. [CrossRef]
27. Weiss, C.; Kobayashi, H.; Gouterman, M. Spectra of Porphyrins. Part III. Self-Consistent Molecular Orbital Calculations of Porphyrin and Related Ring Systems. *J. Mol. Spectrosc.* **1965**, *16*, 415–450. [CrossRef]
28. Knop, J.V.; Knop, A. Quantenchemische Und Spektroskopische Untersuchungen an Porphyrinen. I. Freie Base Porphin Und Metallo-Porphin. *Z. Für Naturforsch.* **1970**, *25*, 1720–1725. [CrossRef]
29. Sundbom, M. Semi-Empirical Molecular Orbital Studies of Neutral Porphin, PH_2, the Dianion P^{2-} and the Dication PH_4^{2+}. *Acta Chem. Scand.* **1968**, *22*, 1317–1326. [CrossRef]